



Microtextural signatures in quartz grains and foraminifera from tsunami deposits of the Portuguese shelf

Missilene Thaşnara¹ · Pedro J. M. Costa^{2,3} · Francisco Dourado³ · Marta Virginia Alves Martins¹ · Lisa Feist⁴ · Piero Bellanova⁴ · Klaus Detheler⁴

Received: 14 November 2022 / Accepted: 7 February 2023

© The Author(s), under exclusive license to Springer Verlag GmbH Germany part of Springer Nature 2023

Abstract

This study presents results from two sediment cores collected on the southern Portuguese shelf attempting to partially fill the knowledge gap of the offshore record of high-energy events. The results were obtained based on description of cores, microstructural analysis of quartz grains, and foraminiferal taphonomy. The lithostratigraphy corresponds to late Holocene sedimentation, with intertidal intercalations of medium sand rich with bioclastic fragments and massive basal contact. In terms of microtextures, a high degree of mechanical marks on the grains associated with tsunami deposition was observed and reflects the high-energy hydrodynamic processes. In depositional terms, the higher presence of quartz grains in these units favors the increase of mechanical marks because grain-to-grain contact is more intense. Additionally, the geomorphological setting of theoring sites controlled the degree and type of mechanical microfeatures observed. Furthermore, post-depositional changes and characteristics of the original sediments source contribute to explain the occurrence of dissolution in units of Geral 23313-02. The foraminiferal taphonomy displayed a predominance of dissolution alteration in the wet surfaces that was more evident in the silty layers. On the other hand, similar to quartz grain microtextural signature, the sandy high-energy units exhibit a slight predominance of physical processes despite the still strong presence of dissolution. The sole presence of foraminifera species from the middle to the outer shelf in some units is an indication that there was little reworking of specimens. This work aims to increase the understanding of dynamics during Holocene high-energy events and to characterize their backwash phases through the different imprints left in the sedimentary offshore record of the Portuguese Algarve shelf.

Introduction

The limitations of data collection and interpretation on the frequency and magnitude of past tsunami events present day studies aiming to define the risks of these phenomena. Therefore, geological archives are keys to reconstruct and understand past histories and dynamics of these events. In this sense, evidence in coastal stratigraphy left by humans allows correlating the parameters of waves and their characteristics with sediment transport and deposition during these events (Costa et al. 2019a).

The study on these extreme events has grown in number and in detail over the last two decades. However, evidence of backwash on the shelf is still little explored compared to onshore deposits. The study by Abraão et al. (2019) in the Tagus delta, on the central western shallow shelf of Portugal, proved that offshore settings have the potential to preserve evidence of tsunami deposits.

✉ Missilene Thaşnara
thaşnara@gmail.com

¹ Departamento de Geologia Aplicada, Faculdade de Ciéncias, Universidade Do Estado Do Rio de Janeiro, Rio de Janeiro, Brazil

² Departamento de Ciéncias da Terra, Faculdade de Ciéncias, F. Theologia, Universidade de Coimbra, Rua Silveira Lima, Univ. Coimbra - P-300-790 Coimbra, Portugal

³ Instituto de Ciéncias da Terra, Instituto Dom Luís, Universidade de Lisboa, Instituto I3, Campo Grande, 3740-000 Lisboa, Portugal

⁴ Institute for Neuroscience and Natural Research, RWTH Aachen University, Fachhochschule 4, 52070 Aachen, Germany

In order to contribute data on offshore tsunami deposits, surveys were conducted in the Algarve shelf (southern Portugal), which revealed not only the record of the 1755 CE tsunami but also of another event, which occurred about 3400 years BP (Reichert et al. 2019). This event was not recorded or preserved in the onshore geological record and led to a change in the definition of recurrence periods of these phenomena for the SW sector of Iberia.

In this study, we investigate the tsunami record in the southern Algarve continental shelf by applying microstructural analysis of quartz grains (U_{238} -Nd-dates fraction) and taphonomic modifications of the *Histerimorpha* test as the main discriminant tools. For this purpose, two offshore sediment cores (GeoR23517-01 and GeoR23513-02—Fig. 1) were studied. With this study, we aim to increase the understanding of dynamics during Holocene high-energy events and to characterize their backwash phases through the different imprints left in the sedimentary offshore record of the Portuguese Algarve shelf.

Study area

The southern Algarve continental shelf is located on the southern Portuguese margin. Its width varies between 3 and 28 km and is characterized by a gentle slope between 0.2 and 2% (Andrade 1987). According to Lopes and Cunha (2010), three domains are identified in this sector: the inner shelf (up to 40 m deep), the middle shelf (between 40 and 90 m deep), and the outer shelf (between 90 m and the platform edge). In turn, the platform edge is well defined and lies between 110 and 130 m deep (Vannay and Mongeau 1991). On it are carved some submarine canyons (e.g., Portimão, Lagos, and Faro canyons), bounded by the marginal plateaus of conjugate origin (Motta 1988). This morphological configuration reflects the clear structural control of the geological evolution of this sector, confirmed with the hydrodynamic of the Mediterranean Water Vessel circulation, a high-density current that circulates through the ocean floor, eroding, transporting, and depositing sediments along the continental slope (Motta 1988; Rybczynski and Barnes 2002; Lopes and Cunha 2010).



Fig. 1 Study area and offshore coring locations

The oceanographic conditions along the southern Algarve coast are typically low energy, with annual average significant wave height (H_{10}) < 1 m and with two predominant wave directions between SW and SE, being the first direction dominant (Costa et al. 2001). According to Manta (1988), the tides on the Algarve coast are regular semidiurnal type, with maximum amplitudes in a single cycle of up to 3.5 m. The current regime is weak on the shelf, with a predominance of drift currents (by wind action) over tidal currents.

The tectonic setting of the SW Iberian margin corresponds to a wide zone of dextral transpressive deformation, associated with the convergence of the Nubian and Eurasian plates (Rusas et al. 2009; Zanchini et al. 2009). This landscape is responsible for significant seismicity that is evidenced by earthquakes and tsunamis, such as the Lisbon earthquake and tsunami in 1755 CE, which devastated the Algarve coast (Gutiérrez et al. 2011), the southwestern Iberian Peninsula, and the northern Atlantic coast of Morocco (Raia et al. 2017). The geological signatures of this event have been very well documented in the works of several authors (Heldring and Andrade 1999; Heldring et al. 1999; Kortekaas and Duijzer 2007; Gutiérrez et al. 2011a,b, 2012). In addition, older tsunamis, which may have affected this region, have also been reported, such as the Tavira tsunami of 1772 CE, among other historical events, compiled in Rapfina and Miranda (2004).

Methods

Sediment cores used in this work were collected by the R/V MITIGOR expedition M152 conducted in November 2018 along the southern Algarve shelf, aiming to study sedimentological data from the 1755 CE tsunami and other possible previous events (Reichert et al. 2019). The specific area of this study is located on the southern Algarve middle shelf. This study focuses on two obtained sediment cores GeoB23512-01 (342,084.643 m E/36°49'01.00 m N) and GeoB23513-02 (343,731.943 m E/4,092,394.269 m N) (Fig. 1). Core GeoB23512-01 and GeoB23513-02 measured 4.67 m and 3.48 m of sediment, respectively, but only samples from the upper parts of the cores were analyzed.

The samples were collected using a vibrocorer system, with a maximum recovery of approximately 3.5 m. GeoB23512-01 was collected at approximately 14 km from the present-day coastline and was recovered at 3.3 m of water depth. In turn, core GeoB23513-02 was retrieved at approximately 12 km from the present-day coast and was collected with 3.0 m of water depth. The horizontal distance between the two core samples is approximately equivalent to 5.3 km. After opening the cores, they were described macroscopically. The units studied in this work were sandy layers interbedded between levels of finer hemipelagic sediments

located in the upper parts of both cores (upper units, within the mainly lithostrophic facies). Thirty-nine samples were obtained from core GeoB23512-01 and 19 from core GeoB23513-02.

The laboratory procedures, applied to the sediment samples, were aimed at separating and testing the fraction greater than 63 µm. Initially, it was necessary to disaggregate the sediments, using a 10% dilution NaOH solution in water for 24 h. Subsequently, the samples were washed with distilled water through a 63-µm sieve. The coarse fraction (> 63 µm) was recovered and taken to the oven at 40 °C. Once dried, the samples were sieved at 0.5-µm intervals. These procedures were carried out in the Micropaleontology Laboratory of the Geology Faculty, Minho University (UELI).

The compositional analysis of the sediments was carried out only on the 220–500-µm fraction. With the aid of a spatula, this fraction was sub-sampled carefully, weighed, and then placed in a foraminifera sorting tray (black checkered plate), and finally analyzed under a Zeiss-Stemi 2000C binocular microscope of the Micropaleontology Laboratory of UELI. The common elements were grouped in three classes (fragments of shells, molluscs, foraminifera, and other organisms), quartz, feldspar, opaque, and others (muscovite and biotite).

For the microtextural analysis (aka. microscopy), quartz grains of the 125–500-µm particle size fraction were analyzed. These grains were selected under the Zeiss binocular microscope Stemi 2000C and prepared for scanning electron microscopy. Mahaney (2002) and Costa et al. (2012a) investigated the statistical representativeness of this analysis and concluded that the minimum number of grains for data to be viable is between 15 and 30 per sample. The analysis of the selected quartz grains was carried out in two laboratories: at the Laboratory of the Centre of Material Technology (CETEM), using the SEM TM3000 Plus-HITACHI, and at the Department of Stratigraphy and Palaeontology of the Geology Faculty of UELI, using the SEM ZEISS model EVO MA 10. The methodology proposed by Costa et al. (2012a, 2014a) was applied to classify the grains. Costa et al. (2012a) suggest the analysis of, at least, five different microtextural characteristics to obtain valid results. This is because a single microtexture is not sufficient to characterize a certain sedimentary environment. Furthermore, these microtextural associations should involve the contrast between marks resulting from mechanical action (pressure marks and fresh surfaces, fractures), typically formed in a context of high energy and shock between particles and features resulting from chemical action (dissolution and adherent particles) usually associated with poor mobility, thus discriminating low-energy environments. There are also features that commonly result from long-term actions, such as grain roundedness.

In the present study, each grain was described according to the microtextural characteristics revealed on its surface (Table 1). After the identification, a semi-quantitative approach was applied to each grain, based on the proportion of the microtexture present on its surface. For this, a scale of 0–3 was adopted, where: 0 (absent), 1 (up to 10% of the grain surface), 2 (10–25% of the grain surface), 3 (25–50% of the grain surface), 4 (50–75% of the grain surface), and 5 (> 75% of the grain surface). Roundness was also evaluated as a complementary attribute, according to Powers (1953), using a rating scale from 0 to 5 (0—very round, 1—rounded; 2—sub-round; 3—sub-angular; 4—angular; 5—very angular).

The focus of foraminifera analysis in this study was the external surface marks that were imprinted in the foraminifera tests. A simplified foraminifera examination was performed on the medium-sized tests. Palaeoecological results should be interpreted with caution due

to the limited size fractions analyzed. The preparation, sorting, and scanning electron microscopy analysis of the foraminifera were conducted at the Institute of Neotectonics and Natural Hazards, KTH Royal Institute of Technology. Samples were sieved to > 63 µm and dried at 40 °C. The dried samples were homogenized and subdivided into smaller sample sizes of approx. 0.01 g. The foraminifera in each sample were counted with a Zeiss Stemi 2000C microscope with 100× magnification. Of these, a minimum of 300 individuals was picked, identified, and stored in Krantz-cells for further investigations. Following Pavia and Tubioli (2017), 300 individuals in the samples are representative for high diversity assemblages of offshore samples. Taxonomic identification up to the rank of genera was based on several reference publications (e.g., Murray 1971, 2006; Bohrnstiel et al. 1996; Kennett and Srinivasan 1983; Lischka and Tappan 1988; Miller and Schmidl 2012). For further identification, images of the

Table 1 Examples for the studied microtextural features

	Penetration marks	These are irregular or angular depressions and are associated with the activity of small or medium-sized organisms.
	Fresh surface	Characterized by the absence of dissolution, precipitation, or weathering marks. In many cases, they are covered with organic deposits or biofilms.
	Fractures	Fracture lines associated with medium-sized tests. Frequently due to impact of hard surfaces. They are produced by mechanical impact.
	Dissolution	Dissolution of (hard) areas indicating the degree of dissolution on the surface of grains. The smooth edges of the solution are the expression of both solution and angular areas and by the formation of cavities.
	Adhering particle	These are characterized by the presence of small aggregates on the surface of the grain grains. Impacted as the result of chemical action.

organisms found at the selected levels were taken by a FE-SEM (Zeiss Supra 55) with the secondary electrons (SE) at a voltage of 3 kV and uncoated in order to assess the conservation of the surface of its tests.

The individuals were classified according to the degree of physical alteration when they presented fragmentation or abrasion, and dissolution marks were used to identify chemical alterations. Analytical criteria were applied in order to establish the degree of alteration. These were based on the works of Pilatczyk et al. (2011; 2012; 2020). Thus, it was considered: (0) when the shells were unaltered, being considered well-preserved; (1) slightly altered; (2) moderately altered; and (3) very altered.

Results

General description of cores

The description of cores was based on macroscopic physical aspects, such as color, type of contact, sediment composition and amount of bioclastic fragments. Based on these visual aspects, units were designated to describe the sandy intercalations present in the cores. Macroscopically, the upper part of GeoB23512-01 (Fig. 2 (I)) is composed of dark green sandy silt and silty material, with intercalations of sand layers (units B1, C1, and D1) that are rich in bioclastic gravels. The basal contacts of the units are clearly erosive or sharp. The units were identified between 81–102 cm (B1), 127–158 cm (C1) and 217–218 cm (D1) below seafloor (bsf) in the referred sediment core. An intercalation of fine grayish sand was observed at the level between 23–38 cm bsf (unit A1).

In the sediment core GeoB23513-02 (Fig. 2 (II)) from the 164 cm bsf to 45 cm bsf, an erosive layer of very fine sand occurs (unit B2). It has a grayish color and features of intense bioturbation occur, which are traces of activity of living organisms such as bivalves and gastropods present in the unit. Overlying this layer, between 45 cm bsf and the top, greenish sandy silt occurs. This silt layer is interrupted by a level of sand rich in bioclastic gravels between 31 and 35 cm bsf (unit A2). This level presents an erosive basal contact.

The sediment composition analysis (Fig. 2c; Appendix 1) revealed that the sandy layers of both sediment cores are predominantly composed of bioclasts and secondarily of quartz, feldspur, and few grains of opaque minerals and micas. It is important to note that units B1, C1, D1, and A2 (bioclastic sand) shows the highest percentage of lithoclastic elements when compared to those observed in unit A1 and B2 (fine sand and very fine sand).

Quartz microtextures

The microtextural attributes of 313 grains from B1 core samples from GeoB23512-01 and 281 grains from B2 core samples from GeoB23513-02 were identified and classified; these results are illustrated respectively in Fig. 2b and c (Appendix 2 and 3). The analysis of SEM images of the microtextures is summarized in Fig. 3.

GeoB23512-01

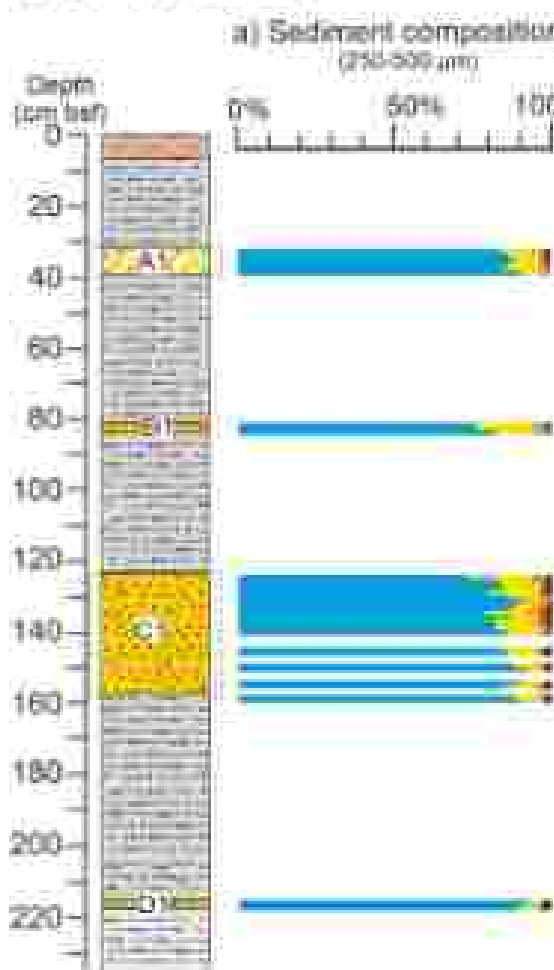
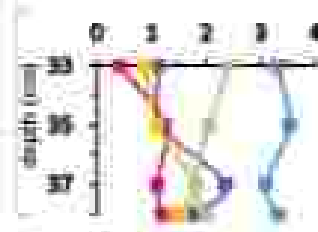
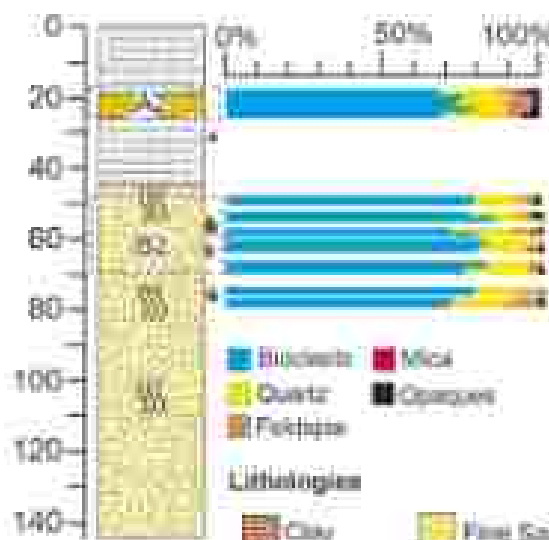
The analysis of the microtextural attributes in this unit were over distributed grain distributions and mean values between units A1 (very fine sand) and B1, C1, and D1 (bioclastic sand). In unit A1, there is an abundance of chemical features such as dissolution (28%) and adherent particles (23%), as opposed to percussion marks, fresh surface, and fractures, which are noticeably less frequent. In terms of mean values of the surface of grains occupied by each microtextural feature, dissolution stands out showing the highest value (mean 3.11 ± 0.17), followed by adherent particles (2.06 ± 0.25). The values of mechanical action marks, such as percussion marks (0.98 ± 0.26), fresh surfaces (0.61 ± 0.28), and fractures (1.21 ± 0.40) are relatively lower in this layer.

On the other hand, in samples from units B1, C1, and D1, it is observed that the microtextural attributes related to mechanical impacts are more frequent and dominant on the surfaces of the quartz grains, especially on the lower and upper limits of the expressive sand layer of unit C1 (127–128 cm bsf and 157–158 cm bsf). Percussion marks, fresh surfaces and fractures present very regular occurrences distributions, with 34% of occurring each. Regarding grain surface luminance, fresh surfaces dominate (1.49 ± 0.21), followed by percussion marks (0.69 ± 0.36) and fractures (2.93 ± 0.31). The features of dissolution (1.56 ± 0.24) and adherent particles (0.94 ± 0.18) occur more distinctly here.

Regarding roundness, in the bioclastic sand units (B1, C1, and D1), the analyzed grains exhibit an average of 2.78 ± 0.26 , characterized as sub-angular. At the same time, when the very fine sand occurs (unit A1), the mean values are 3.26 ± 0.21 ; therefore, the grains are considered sub-angular to sub-rounded.

GeoB23513-02

In sediment core GeoB23513-02, the distribution of microtextural features did not show significant differences along the vertical analysis performed. The occurrence probabilities of microtextural features differ by 1% or 2% throughout the samples analyzed. Dissolution dominates, followed by fresh surfaces, percussion marks, and fractures, while adherent particles are the least frequent. In unit A2, considering the

I - GeoB23512-01**Microtextural Analysis****b) Relative frequency****c) Mean****II - GeoB23513-02****Base Boundaries**

Concretion
Fissure

Fluviatile
Institution

Fig. 2 Results from sediment cores Gec0233C1-01 and Gec0233C1-02. **a** Morphologic (macroscopic) variation. **b** Micromorphological frequency. **c** Average value of the semi-quantitative micromorphological classification for the micromorphological dominance on the grain's surface

mean values of grain surface dominance. Fresh surfaces (2.46 ± 0.18), percussion marks (2.10 ± 0.71), and dissolution (1.89 ± 0.25) are the most relevant microtextural features.

In unit B2, the dissolution coverage is clearly more expressive (mean 2.44 ± 0.53) in relation to the other microtextured attributes. In turn, regarding micromorphological dominance, incipient marks are more discrete, with averages ranging between 0.96 and 2.00 . Incisiveness presents values of 2.14 ± 0.19 in unit A2 and 2.82 ± 0.25 in B1, respectively sub-angular to sub-rounded.

Foraminifera analysis

A total of 846 SEM images of foraminifera individuals were analysed (Fig. 4) and 31 species identified (Appendix 4), of which the most frequent are *Reticularia pseudopunctata* (Hinze-Alten and Hartland 1930), *Cribromytilus peroni* (van Veenhoven 1957), *Globigerina bulloides* (d'Orbigny 1836), *Nodosaria jahnsi* (Richard & Möll, 1799), *Quinqueloculina stellari* (Lodderick & Tappan 1957), *Solenites punctatus* (Wright 1947), and *Globigerina falconensis* (Rhee 1959). The foraminifera were retrieved from 32–34 cm, 34–39 cm, 62–66 cm, and 74–78 cm bsl from Gec0233C1-02 (Fig. 2 (II)). Regarding abrasion, it was observed that 24% of the foraminiferal tests are unaltered, whereas the remaining 76% present some level of alteration. Individuals showing fragmentation, breakage, and abrasion marks were classified with physical alteration and those showing dissolution marks with removal of the surface were classified with chemical alteration.

The results show that the type and degree of alteration differ between the sandy and the silty layers. In the silty layer, between 32 and 34 cm bsl, it can be observed that dissolution occurs more frequently, with a percentage of 64% (average 1.42), exhibiting small alterations to almost total destruction of the specimens. On the other hand, the effect of physical alteration in this interval occurs in only 36% of foraminifera with mean values of 1.00.

In contrast, the intervals 34–39 cm, 62–66 cm, and 74–78 cm bsl of unit B2 exhibit a slight predominance of tests worn by physical abrasion, with percentages varying between 53 and 56% and with degrees of alteration between 1.11 and 1.34. The marks of alteration by dissolution are less

abundant in this layer and the average values vary between 0.79 ($34\text{--}39$ cm bsl) and 1.10 ($62\text{--}66$ cm bsl).

Discussion

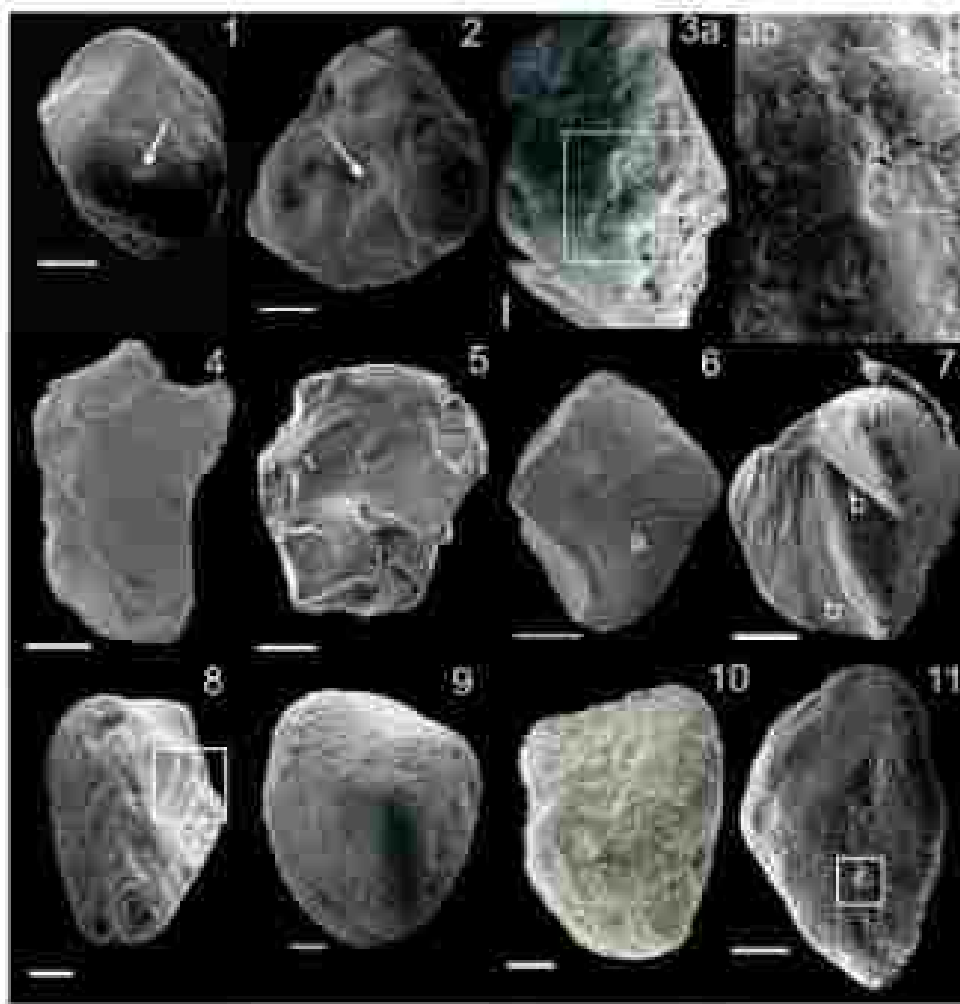
Lithostratigraphic interpretation

Based on the data obtained, high-energy events were detected, responsible for the deposition of units with contrasting characteristics in the stratigraphy (B1, C1, D1, and A2). Especially the C1 and A2 units, due to their largest expressions of approximately 30 cm and 5 cm, respectively, are interpreted as products of high-density flows from the coast to the sea (probably caused by the tsunami backwash) in the middle shelf of southern Portugal, generating the sudden incision of coarse materials rich in shell gravel, interrupting the low-energy sedimentation regime. The richness in shell fragments is one of the attributes that can characterize tsunami deposits and is a good marker of the high-energy involved in sediment transport, according to Gelli et al. (1998, 2000, 2010). The presence of bioclastic sand layers with intense fragments and shell gravel suggests, therefore, that they were probably deposited under conditions of higher hydrodynamic energy.

The base between the high-energy deposits (C1 and A2) with the underlying layer shows an erosional contact and indicates a high tensile force caused by (tsunami) flow recession or backwash, reducing the genetic difference between both layers. Frosty surfaces were observed in deposits from the 1755 CE tsunami on the southern Portuguese coast and are commonly used to define the lower limit of these deposits (e.g., Hinzen and Antunes 1999; Kortekämä and Dawson 2007; Costa et al. 2012a; 2014b).

Tsunami effects in the offshore sector were addressed by Abrantes et al. (2009) in the Tagus delta, in the SSW stratigraphic record of the shallow shelf of Portugal, referring to the events of 1969 to 1755 CE. Also, in the offshore sector of the SSW Iberian Margin, Gracia et al. (2010) recognized seven turbiditic events with erosive bases, linked to instrumental and historical earthquakes, tsunamis, and paleotsunamis. The results obtained in other zones close to the area of this study, in the expedition R/V METEOR M152/1 (Reuchert et al. 2019), show high-energy deposits with erosive bases and coarse-grained composition (well-sorted medium sand), at depths of 16–25 and 122–153 cm bsl. These deposits were radiocarbon and OSL dating, associated respectively with the 1733 Lisbon tsunami and another event that occurred at about 3400 years cal BP. These works prove that the

Fig. 1 SEM quartz grains imagery with Scale bar: 100 μm : 1–3c: Fresh surfaces nearly totally erasing the grain; 4–7: grains with fresh surfaces; 8) conchoidal fractures; 9) linear fractures; 8: grain with strong dissolution features presenting lacunae (highlighted); 9: grain with high degree of dissolution; 10–11: grains where chemical features dominate – e.g., adhering particles in the grain's surface



affidence vector has the potential to provide evidence from high-energy events.

Microtextural analysis

High-energy deposits present intrinsic peculiarities that are sensitive to their depositional environment. This is clear when comparing the data obtained from sediment cores GEOF23512-01 and GEOF23513-01. Considering GEOF23512-01, it is notable that the quartz grains of unit A1 (33–38 cm bsl), present contrasting microtextural characteristics with units B1, C1, and D1 (81 cm, 127–138 cm, and 218 cm bsl).

In unit A1, the high proportion of chemical marks is attributed to post-depositional changes, such as diagenetic processes or bioturbation. It has been described that low-energy environments are more susceptible to chemical weathering (Mahaney 2002; Viss et al. 2014). The abundance of adherent particles in these grains also justifies diagenetic traces (Mahaney 2002). Furthermore, the high

mean value for the presence on the surface of grains suggests a calm and long residence time in the environment, which would be only possible in a low-energy marine depositional environment.

In contrast, units B1, C1, and D1 present higher values of mechanical marks, indicating stronger hydrodynamic processes during deposition (Mahaney 2002). The increase of permeation marks is promoted by erosion and incorporation of sediments during the initial phase of innumi backwash. According to Costa et al. (2012a), this feature is linked to the high concentration of sediments in the water column, forcing intensive contact between grains. This justifies the maximum mean values found at 127–138 cm bsl, at the base of unit C1. Moreover, this scenario promotes the highest fracturing of the grains at this level (127–138 cm bsl); in fractures are related to strong impacts on the grain surface (Viss et al. 2014), whose incision size reflects the energy associated with these formations (Talay 1979; Mahaney 2002).

The presence of fresh surfaces on the quartz grains of units B1, C1, and D1 in GEOF23512-01 corroborates



Fig. 4 SEM imagery of ammonites tests with scale bars of 10 μm . **(1, 2)** *Reticularis pilosa* Hermann, 1802; **(3)** *Alliotropis virens* Parker, 1932; **(4, 5)** *Bivalvia subcarinatus* Couthouy, 1822; **(6)** *Nemirovskia subtilis* Lischke & Tappan 1933; **(7, 8)** Unaltered; **(9)** *Neuroleptites plicatus* Le Cajun, 1959; **(1–3)** Wet preserved specimen; **(4–6)** Aboral physical tests; **(7–9)** Images showing the degree of chemical alteration. The increase in the degree of change occurs in the direction of the arrow

strong hydrodynamic processes immediately prior or during deposition. Their occurrence results from violent collisions to the point of extracting large percentages of the grain surface generating fractures and fresh surfaces. According to Costa et al. (2012a), the low concentration of sediments in the water column should favor the increase of these features, because the particles would have more space in the aqueous medium, and thus, the impact velocity would be higher and more energetic (higher kinetic energy). The highest mean values of fresh surfaces were detected at the top of unit C1, between 127 and 129 cm bsl. The lower sediment concentration at the top of the deposit can probably result from the last backwash phase (before settling of the fine sediments), as erosion and resedimentation of sandy sediments were intensely caused by the previous waves. A slight increase of mica grains at the top of the deposit, between 127–131 cm bsl, reinforces this reasoning and might attest to the product of

the final backwash phase. This is because the properties of these minerals (their density and habit) give them more heterogeneity in the water column, being deposited, in lower energetic conditions.

Regarding the microstructural results obtained from GRL23113-02, it is noted that the differences between the mechanical and chemical attributes are not statistically significant between unit A2 (21–25 cm bsl) and B2 (48–68 cm bsl). This is due to the occurrence of dissolution marks on the grains in unit A2. It is worth noting that at the base of unit A, fresh surfaces and porosities marks exhibit an increase, whereas at the top fresh surfaces occur with higher average values than the other attributes. Similarly, the same reasoning can be applied to units B1, C1, and D1 of core GRL23113-01, and one can infer that the concentration of sediments in the water column influences the generation and intensity of mechanical microfeatures. Regarding quartz grains of unit B1, the mechanical marks occur discretely, without very contrasting mean values.

Regarding the average degree of roundness, this characteristic was not significantly different among the grains analyzed from both sediment cores. In the bioclastic sand layers (units B1, C1, D1, and A2) the grains are sub-angular, while in the fine and very fine sand layers (respectively A1 and B2), the average values correspond to grains between sub-angular and sub-rounded. It is considered that the brief duration of the event did not generate more notable changes in the grain shape.

The processes responsible for producing chemical features and mechanical impact marks do not share similarities (Muhunay 2002; Costa et al. 2012a; Von et al. 2014). Therefore, it is considered that the dissolution features on the grains in units A2 and B2 of GRL23113-02 are related to post-depositional changes or poor resurfacing (preferentially of coarse sediment features). There are also paleofloods submerged at around 40 m of water depth, according to the continental shelf surface sediment chart (Hydrographic Institute 2009). Dunes have been commonly described with strong dissolution features (Muhunay 2002; Costa et al. 2012a; Von et al. 2014). Thus, it is possible that the quartz grains analyzed already held chemical imprint which supports the lack of microtextural heterogeneity in core GRL23113-02. Differences in recognizing microtextural signatures related to tsunami events were reported in Kuijpers et al. (2012a), who investigated sediments from the 1755 CE tsunami on the southern Portuguese continental shelf in the vicinity of Faro. The authors detected only a small increase in porosity marks, and that a possible change in grain size distribution after the 1755 CE event may have influenced the signature in the outer shelf sediments recorded.

The compositional analysis of only particles of the 250–500- μm fraction somewhat favors reaching more

conclusive interpretations. However, it indicates the non-pelagic elements that can be related to higher hydrodynamics. Although the biogenic elements dominate in more than 70% of the samples from both cores, it is noteworthy that there are levels in the bioclastic sand layers (units B1, C1, D1, and A2) where there is an increase in the percentage of quartz grains. This may indicate changes in hydrodynamics that are reflected in the composition of the sediments. The incorporation of quartz grains in the water column, therefore, induces higher mechanical stress during collisions, since these materials have a higher density than the biogenic elements, which is translated by the formation of a higher number of mechanical microstructures.

Another important factor that argues for the microstructural differentiation exhibited in the is the configuration of the local bathymetry. Turbulent backwash flows return to the sea causing erosion and re-deposition of sediments with velocities influenced by the submarine topography (Bawden and Stewart 2017; Sessaar et al. 2008). In this study, GeoB23312-01 is located in the vicinity of the Portimão canyon, which causes an 8-km-long incision in the shelf (Dias 1987). This pronounced structure may act as an "oulet" through which flow transports and deposits sediments with higher velocities. From a hydrodynamic point of view, the flow velocity is directly related to the depth of the water column, calculated using the formula $v = \sqrt{gk}$, in which g is the acceleration of gravity and k is the depth (Barman 2019). Thus, the wave travels faster in steeper areas than in a shallower area once the work of the bottom friction begins to act on the continental shelf. For this reason, the energy of the backwash flow on the Portimão canyon and its vicinity played a determining role in the higher degree of sediment eroding, having a direct effect on the final configuration of the deposit and justifying the microstructural and compositional lateral variation observed between the two sediment cores studied. This reasoning supports the presence of more mechanical marks in GeoB23312-01 than in GeoB23313-02.

Recognizing microstructural signatures in tsunami deposits in the offshore context is not a simple task, as it is a dynamic environment open to processes that impair the preservation of these features. However, we proved that through the application of this technique, we were able to distinguish signatures that allow identifying high hydrodynamic processes, such as tsunami backwash, mainly in the GeoB23312-01 core. Despite the challenges in establishing a vertical trend along the tsunami deposit of GeoB23313-02 (due to the strong presence of dissolution), it is possible to detect at the base and top of the A2 deposit (21–23 cm bsl) no increase in mechanical marks, especially fresh surfaces. Many local factors can influence the formation of such features, such as the energy of the event, the source and sediment concentration, and also

post-depositional processes, as already reported here. Furthermore, it is observed that the sedimentary composition plays an important role in the formation of microstructural signatures.

Foraminifera taphonomy

Preservation and taphonomic features in foraminiferal tests can reveal information of tsunami flow velocity, sediment concentration, abrasion, and post-depositional environmental processes (Manni et al. 2009). In this study, the occurrence and degree of abrasion (Fig. 4 (7–9)) observed in tests from the silty layer (32–34 cm bsl) of GeoB23313-02 may be a result of the low-energy environment. According to Keefer et al. (1992) these environments promote a high deposition of organic matter in the sediments which can favor boring fauna to rework the organic matter, producing acid-saturated microenvironments that lower the pH of the water, triggering chemically altered shells (Cattley and Halleck 1968; Murray 1999; Walter and Barron 1997).

In unit B2 (34–39 cm, 62–66 cm, and 74–78 cm bsl), a combination of physical and chemical processes occurs with a slight predominance of physical alteration marks, some of them often of difficult recognition (Fig. 4 (4–6)). The occurrence of physical alteration marks can be attributed to an increase in the energy of the environment, therefore providing deposition of particles in the very fine sand fraction, in contrast to the overlying low-energy silty layer. However, the resulting transport energy was not sufficient to generate more intense abrasion and fragmentation, possibly because in these very fine sand layers, there is a dominance of less basic components in about 80% of the sedimentary composition. The experiments by Marin and Lüder (1991) prove that even in high-energy environments, the foraminifera tests are not usually altered by abrasion caused by friction with carbonate sediments, as occurs in mixed and siliciclastic environments.

Moreover, the species identified in this study are from the middle to the outer shelf. It is interpreted that these individuals did not undergo relevant reworking triggered by the phase tsunami inundation and backwash. Gómez-Breyuglio and Hochmesser (2014) attest that the poor preservation of foraminifera shells by abrasion is a consequence of transport processes. In turn, Quimada et al. (2016) verified the presence of burkenfultered marine species, however, in seismic deposits as a product of the highly energetic transport of the initial tsunami inundation phase.

In this work, it is emphasized that the dissolution characteristics of the quartz grains of unit B2 of GeoB23313-02 are interpreted as a characteristic inherited from the sedimentary context, or even a result of

post-depositional changes. In fact, bioturbation imprints are present in this unit and have the capability to trigger the occurrence of dissolution in the bioclastic unit (Walker and Burton 1999; Parsons and Brett 1997; Koster et al. 1992).

Conclusion

The sedimentary characteristics observed in the studied cores allowed the detection of high-energy events in the sand units III, CI, D1, and A2, mainly regarding the units CI and A2 due to their significant expressions in the stratigraphy. The set of contrasting features in the lithofacies, such as erosive basal contact, compositional characteristics with abundant bioclastic gravel, as well as erosive and taphonomic data, allow interpreting them as a result of a high-density flow from the coast towards the sea, caused by the tsunami backwash.

From the microtextural analysis, it was discerned that the GeoR22S12-01 core registered a higher frequency and degree of mechanical marks in the bioclastic units II, CI, and D1. This abundance indicates that these attributes were sculpted in a high-energy hydrodynamic environment. On the other hand, in the GeoR22S13-02 core, despite high values of mechanical action at the base of the unit considered taphogenous (unit A2), there was little micromechanical contrast with the lower unit II, due to the stronger presence of dissolution in the grains of quartz in A2. It is very likely that in addition to the concentration of sediments in the water column, the local bathymetry and the paleoepic flow play an important role in the imprinting of the microtextures, since the backwash was channeled more intensely through the Portillo canyon, thus favoring the generation of mechanical impressions mainly in the GeoR22S12-01 sounding (Fig. 3 A and B).

Sediment composition also played a role in the generation of microtextures. This is due to the slight increase of quartz

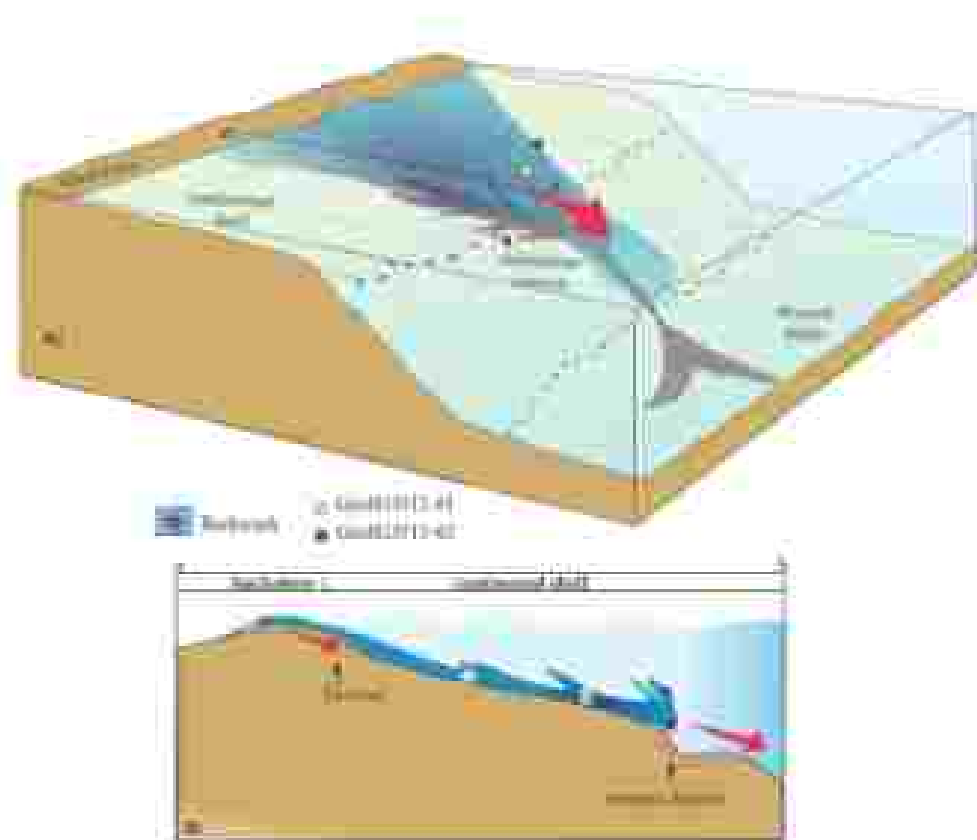


Fig. 5 Conceptual model of the backwash dynamics: A. Diagram illustrating approximately the position of the cores in relation to the Portillo canyon. The backwash flow constrained in the canyon reaches higher intensity as the depth increases. As energy is proportional to velocity, the flow channeled through the Portillo canyon generates more generation of mechanical marks (erosion marks, fractures, and fresh surfaces) on the quartz grains of the GeoR22S12-01 core, which is more influenced by this energy than the core GeoR22S13-02. B. The schematic profile a-b illustrates the generation

of mechanical microtextures, controlled by the concentration of sediments in the water column during the different stages of the flow. The backwash causes erosion and subposition of sediments in the sea, is I, the high concentration of sediments carried by the initial waves favors the formation of fractures and pitting marks. When most of the sediments were transported by previous flows, the low concentration of sediments in the water column, is II, generates more energetic collisions, favoring the predominance of fresh surfaces

grains isolated from the water column by erosion triggered by the back wash flow. This is enough to magnify the mechanical shock between the quartz grains in the bioclastic units. Furthermore, post-depositional changes and original features of the sedimentary source may help to explain the lack of disseminated heterogeneity in Gc1dCTM13-02.

From the results of leptoconcho, it was evident that in the silty layer, the foraminifera seem essentially altered by dissolution. On the other hand, in the sandy unit, there is a slight increase in the test dissolution, despite that the occurrence of dissolution is still noted. The exclusive presence of nucifer foraminifera (medium to minor platform) in the sandy units attests that there was only reworking of sediments close to the source. The leptoconcho analysis needs a more vertical approach in the cores; a deep paleoecological study of these specimens is suggested.

It is not possible to detect the deposition of benthos with a single isolated proxy, but the combination of evidence obtained in this study, added to the local sedimentological context and the results obtained in the literature, allowed us to presume that the C1 and A2 units are related to the back wash dynamics of benthos. Finally, the continuation of investigations of the offshore sedimentary record of the SW sector of Portugal is fundamental to expand the understanding of tsunami events in the past, as well as to understand their risks in the future.

Supplementary information The online version contains supplementary material available at <https://doi.org/10.1007/s00367-021-00343-0>.

Acknowledgements The authors thank the Coordenação de Aperfeiçoamento de Pessoal de Nível Superior (CAPES) for the financial support for the scholarship grants. We also express our thanks to Professor Luis C. Bernardo for the technical support during the SHM microscopy at the facilities of CHTM. Likewise, we want to acknowledge the SHM utilization (DHPA, UHEIA) under the responsibility of Sírgio Borgesma. The authors are deeply grateful to the research and technical crew under the command of Captain R. Hammacher from RV MARYSE – MUS2. Fundação para a Ciência e Tecnologia (FCT) is acknowledged for its funding of project Centro INET/C/TM/2013/03941/2017.

Author contribution This paper was developed from the thesis of master of Maxime Ythamer. Elisa Reichené – project leader, Pedro JM Costa and Francisco Oliveira – conceptualization, methodology, Luis Faria – preparation the sediment samples, Pedro Bettencourt – scanning electron microscopy of the foraminifera; Maria Virginia Alves Marques – identification of species foraminifera; Maxime Ythamer was responsible for analysis and interpretation, and drafted the figures of the manuscript. The first draft of the manuscript was written by Maxime Ythamer and all authors contributed or revised: sections of the manuscript and made substantial contributions to the conception of the work.

Funding This work was supported by the Fundação para a Ciência e Tecnologia (FCT) project Centro INET/C/TM/2013/03941/2017 and by Coordenação de Aperfeiçoamento de Pessoal de Nível Superior (CAPES) by grants to Maxime Ythamer (B8813/S02390/2020/00).

Data availability All data generated or analyzed during this study are included in this published article and its supplementary information files.

Code availability Not applicable.

Declarations

Competing interests The authors declare no competing interests.

Other approval Not applicable.

Consent to participants Not applicable.

Consent for publication Not applicable.

Conflict of interest The authors declare no competing interests.

References

- Almeida P, Alc. Piquet U, Lebreiro A, Voukler A, Suttorp H (2016) Sedimentological record of tsunami on shallow-shelf areas: the case of the 1755 AD and 1775 AD tsunami on the Portuguese Shelf off Lisbon. *Mar Geol* 369(3–4):203–213. <https://doi.org/10.1016/j.margeo.2017.11.004>
- Antracite C (1990) Constituição de barreiras na Baía Formosa (Algarve - Portugal). Universidade de Lisboa para obtenção do grau de Doutor em Geologia, na especialidade de Geologia do Ambiente, Departamento Geologia da Faculdade de Ciências da Universidade de Lisboa, Lisboa, 603 p.
- Baptista MA, Mendes PM (2009) Review of the Portuguese catalog of tsunami. *Nat Hazards* 50(1):25–42. <https://doi.org/10.1007/s11064-008-9223-3>
- Burnas SK (2020) Physics of tsunami: generation, propagation and rise of the ocean. *Int J Oceanic Oceanogr* 14(1):1–16. <https://doi.org/10.3392/ijooceanogr.1.10201>
- Browne WH (1936) Age, correlation, and bathymetry of the west Tocuyo (San Lorenzo) and Puerto Pampanga, eastern Falcon, Venezuela. *Bull Am Paleontol* 30:67–221
- Bronkhorst E, Glasmacher C, Wyllman S, Wright R (1990) Ages of fossil shell accumulations of the Southeast Atlantic. De W. Junk bv Publishers, The Hague, 247 pp. pt. II
- Bruna A, Hohmann J (2011) Flow in tract in shallow water hydrodynamic: the large benthic foraminifera system. *Mar Micropaleontol* 81(1–2):3–26. <https://doi.org/10.1016/j.marmicro.2011.07.004>
- Costa PM, Antracite C, Dawson MC, Matusev WC, Pachiaudi MC, Pavia R, Taborda W (2012a) Microtextural characterization of quartz grains transported and deposited by tsunami and storms. *Sedimentology* 57(5–7):1603–1619. <https://doi.org/10.1002/sed.20113>
- Costa PM, Dawson MC, Ribeiro RD, Braga M, Dinisso F, Boaventura L, Antracite C (2012b) A review on modern tsunami deposits along the Atlantic coast. *Earth-Sci Rev* 112:397–421. <https://doi.org/10.1016/j.earscirev.2012.07.001>
- Costa M, Silva R, Vicente J (2007) Constituição para o estudo sistemático das espécies foraminíferas marinhos portuguesas. 2º Seminário Português de Paleobiologia Costeira e Estuarina, 20
- Costa P, J. M. Antracite C, Ferreira M, Oliveira M, Lopes V, Dinisso A, ... Josemaria J-M (2012b) A tsunami record in the sedimentary archive of the central Algarve coast, Portugal: characterizing sediment, reconstructive sources and inundation paths. *The Holocene* 22(9): 939–944. <https://doi.org/10.1177/0950093812449477>

- Costa TJM, Andrade C, Freitas MDC (2014) Assemento macroscópico de praias, anfíbios e répteis marinhos. O desastre da tsunami de 1755 na Baía do Rio em caso de ressaca. Prospecção de material pertigoso: abrangência sobre o Oceano Atlântico. *Terra*, 77–56

Costa TJM, Andrade C, Freitas MDC (2014b) Another macroscopical approach, procedures and characteristics macrobióticas de praias de quartzo. *Prospecção de materiais pertigoso: abrangência sobre o Oceano Atlântico*, 19–36

Cotter TI, Rabych P (1988) Test surface degradation in *Arenites argillacea*. *J Microscopist Res* 18(3):361–367. <https://doi.org/10.1007/BF02434771>

Dawson A, Stewart J (2007) Tectonic processes. *Prog Phys Geogr Earth and Environment* 31(6):575–590. <https://doi.org/10.1177/0309133207080602>

Dias JMA (1947) *Geodinâmica hidrodinâmica e evolução morfológica da praia-fundo continental portuguesa submersa*. 1907, p 364. Dissertação de doutoramento, Faculdade de Ciências, Lisboa

Dias J, Rosa PM, Torreiro P, Soutar W, Rossetti O, Guedes M-A, Oliveira A (2011) Are submergence zones invading the Atlantic? Evidence from the eastern Iberia margin. *Glob Geol* 4(10):839–842. <https://doi.org/10.1190/GEO2010.1>

Faria F, Taborda H (2002) Confidence limits of species proportions in microfaunal assemblages. *Mar Micropaleontol* 46(2):169–174. [https://doi.org/10.1016/S0377-8398\(02\)00021-4](https://doi.org/10.1016/S0377-8398(02)00021-4)

Fischer L, Muñiz JP (1990) Testacea macroscopio, abelhas minota e gasterópteras Argonauta et Nudibranchia, w/ novas distâncias e descrição. A. Fischer. *Wiss. 10* e 113, 74

Gill JR, Cooper M, Sanderson V, Cochran D, Shaw P (1997) Possible tsunami deposits from the 1926 earthquake, North Island, New Zealand. *Geol Soc* 146(1):357–374. <https://doi.org/10.1144/gsj.146.1.0121> (London, Special Publications)

Gill JR, House HL, Jones SJ, Hayward BW, Cochran U, McLean W, Moleski MS (2000) Evidence for an earthquake and tsunami about 3100–3000 yr ago and other catastrophic coastal inundations recorded in a coastal lagoon, New Zealand. *Mar Geol* 176(1–2):211–240. [https://doi.org/10.1016/S0025-2770\(00\)00076-1](https://doi.org/10.1016/S0025-2770(00)00076-1)

Gill J, House SJ, Nichols SJ, Chapman-Gill C, Harrold M, Somer J (2000) Multi-proxy records of megathrust coastal seismicity, New Zealand. *Geomorphology* 31(3):349–362. [https://doi.org/10.1016/S0169-5936\(00\)00005](https://doi.org/10.1016/S0169-5936(00)00005)

Gracia P, Vicente A, Peñalba C, Álvarez A, Soler A, Palma R, Garrido-Jiménez J, López-Sáez J, Goldring C (2010) Holocene-eustatic record offshore Portugal (SW Iberia): using molluscan paleoecology to a new perspective sample. *Quatern Sci Rev* 29(8–10):1156–1172. <https://doi.org/10.1016/j.quascirev.2010.01.010>

Harris-Aiken E, Hartland A (1930) The invertebrates of the pseudotidal Duncraig, L.J.H. Munro. *Proc Roy Soc Edin* 50:46–84. <https://doi.org/10.1111/j.1463-9986.1930.tb00175.x>

Higgs R (1979) Coarse-grain surface lenses of Mytilus-Common mussels from the Labrador and Western Greenland continental margin. *SEPM J Sediment Res*, 46. <https://doi.org/10.13063/2373-7234.1447>

Hinsby B, Andrade C (1990) Sedimentation and hydrodynamic processes associated with the tsunami generated by the 1755 Lisbon earthquake. *Quatern Int* 26(1):27–38. [https://doi.org/10.1016/0108-9347\(90\)90014-3](https://doi.org/10.1016/0108-9347(90)90014-3)

Hudson RA, Andrade C, Dawson AG (1990) Sedimentary processes associated with the tsunami generated by the 1755 Lisbon earthquake on the Algarve coast, Portugal. *Phys Chem Earth* 13(1–2):57–63. [https://doi.org/10.1016/0264-9069\(90\)90014-4](https://doi.org/10.1016/0264-9069(90)90014-4)

Hwang H (1947) Measurements in the Gulf of Finland and the Skagerrak. *Zoologika Natura*, 26, 1–128

Hydrographic Institute Ludwig (2009) Surface sediments of the Portuguese Continental Shelf. Chap. – S23 T10. Clube São Vicente da Guarda. Report, v. 1. 130–600, 77–84

Kempton JP, Scherzer MS (1980) *Nearshore planktonic foraminifera: a phylogenetic atlas*. Hutchinson Ross, New York, p 261

Kurthkaia S, Dawson AG (2007) Diatomaceous facies and storm deposits: an example from Martinhal, SW Portugal. *Sediment Geol* 200(1–4):206–221. <https://doi.org/10.1016/j.sedgeo.2007.01.004>

Koster H, Martin RH, Koster WD (1992) Experimental analysis of abrasion and dissolution resistance of modern red algal bioherms: implications for the preservation of biological carbonates. *Petrol Geol* 12(3):244. <https://doi.org/10.2377/pg.12.3.244>

Küller W, Drago T, Veiga-Pereira C, Silveira PV, Magalhães V, Moreira A, Lopes A, Rodriguez AI, Schmidt K, Ferreira P, Baptista MA (2010) Exploring sediment resistance evidence of the 1755 CE Tsunami (Portugal): implications for the study of older storm-induced deposits. *Micropal* 16(9):771. <https://doi.org/10.1190/micropal.2010.0472>

Lambach AR, Tappin D (2003) Studies of Arctic bioherms. *Sedimenta Mariana Microbiologiae* 12(1/2):1–150

Lambach AR Jr, Tappin D (1998) *Foraminiferal micro- and their classification*. Van Nostrand Reinhold, New York, p 791

López PC, Costa PP (2010) The Algarve continental shelf and adjacent provinces: a geomorphological analysis. *Geólogos Geopatologos: Estudos Investigacione e Sua Utilizaçao* 1: 479–500

Maloney MC (2002) *Atlas of sand grain-size textures and applications*. Oxford University Press, New York

Marzo B, Sauer J, Dimonie-Holmes D (2000) Tectonic sediments and their benthic faunal associations. *Earth Sci Rev* 46(2/3):279–309. [https://doi.org/10.1016/S0013-092X\(00\)00007](https://doi.org/10.1016/S0013-092X(00)00007)

March RH, Loder WD (1991) The taphonomy of burrowing bivalves in soft-sediment environments: implications for the formation of fossiliferous assemblages. In: Dawson SK (ed) *The process of fossilization*. Columbia University Press, New York, p 170–192

Mikell Y, Schmidt G (2012) A diatomoclastic guide to modern benthic shell accumulations of the western Mediterranean Sea. *Paleoceanol* <https://doi.org/10.2389/paleo.2012.07271>

Monteiro OS (2010) *Carta das Sedimentações Superficiais Nortenhas Ispécie de Fozes SED 7 e 8*. Caldeira S, Vicente do Rio Gaúcho, Instituto Hidrográfico, Lisboa, Portugal

Murray JW (1970) *Atlas of British marine benthos*. Elsevier Educational Books Ltd, London, p 344

Murray JW (1980) Benthopelagic distribution of calcareous benthifauna in shallow shelf–water sediments. *Mar Micropaleontol* 4(1–2):177–211. [https://doi.org/10.1016/0377-8398\(80\)90007-3](https://doi.org/10.1016/0377-8398(80)90007-3)

Murray JW (1986) Faunistic and ecological distribution of calcareous benthifauna in shallow shelf–water sediments. *Mar Micropaleontol* 11:217–221. [https://doi.org/10.1016/0377-8398\(86\)90007-3](https://doi.org/10.1016/0377-8398(86)90007-3)

Orsiere AD (1974) Tafemas mitologicas de la clavada Capitópolo. *Actas das Reunões Naturais* 7–9: 146:245–318

Pearce KM, Brett CE (1991) Taphonomic processes and fauna in modern riparian ecosystems: an activity-based perspective on fossil assemblage preservation. In: DAWSON VAN, S.K. (Eds.). *The process of fossilization*. Columbia University Press, p 22–43

Pilarczyk JE, Rosenthal DG, Rybcyzk D, Schwartz HP, Dziedzic JV (2011) Assessing artificial埋藏物的 distribution as an overwash indicator in the Lapine, Northern St. Olaf, Mar Micropaleontol 60(1–4):41–72. <https://doi.org/10.1016/j.micropal.2011.06.001>

Pilarczyk JE, Rybcyzk D, Rybcyzk D, Schwartz HP, Dziedzic JV (2012) Sedimentary and environmental evidence of the 2011 Tohoku-oki tsunami on the Seattle coastal plain, Japan. *Int Geol Rev* 54(1–2):78–99. <https://doi.org/10.1080/00206813.2012.686011>

Pilarczyk JE, Saito Y, Matsumoto D, Kusumoto Y, Nishida N, Rybcyzk D, Rybcyzk D, Schwartz HP (2016) Determining sediment persistence for tsunami deposits using distributions of grain size and benthofauna from the Kujukuri coastline and shelf, Japan. *Sedimentology*, 63(3):1333–1350. <https://doi.org/10.1111/sed.12781>

- Powell, J. (1923). A new roundness scale for sedimentary particles. *SRPM, I Sediment Res.*, 23, <https://doi.org/10.1007/BF02473673>.
- Quintino M, Costa PM, Faia P, Chapo T, Henke N, Andrade C, Freitas MHC (2016) The Alentejo (SW Portugal) sediment transport interpretation based on the study of Holocene sandstones. *Quatern Int* 406:123–138. <https://doi.org/10.1016/j.quaint.2015.12.029>
- Riedelauer K, Von A, Foss L, Costa PMM, Schwabhauser J, Schütze H, Jem R, Riecke A, Hahn-Petersen K (2019) Lutus 1.725: Creazzo n° M1527, 82, 11, -14, 11, 2018, Funchal (Portugal) – Handbuch (Almada) für M1527/82: Herkunft (Nr. M152, pp. 1–36). Gattendorfer Forschungsgesell., <https://doi.org/10.2231/fn/m152>
- Rifkin P, Harari ED (2013) Microscale patterns in the Cape São Vicente (Western Peninsular) aggrading region. *J Geophys Res*, 118(10):1–10. <https://doi.org/10.1029/2010jc006450>
- Rivas PM, García JC, Terrón P, Varela V, Muñoz L (2000) Morphometric characterization of major bathymetric discontinuity in the Gulf of Cadiz (Africa–Iberia plate boundary): Insights from acoustic-modelling experiments. *Mar Geod* 23(1–4):13–47. [https://doi.org/10.1016/S0309-200X\(00\)80001-1](https://doi.org/10.1016/S0309-200X(00)80001-1)
- Rivas P, Rodríguez-Vidal J, Abad M, Chaves LM, Carrascosa MC, Muñoz M, Rodríguez-Llanes JM, Gómez-Torrealba P, Iglesias T, Sosa E, Townsend A (2017) Sedimentological and geomorphological controls of Holocene transients in southwestern Spain: an approach to establish the recurrence period. *Geomorphology* (Amsterdam), Netherlands 285:97–104. <https://doi.org/10.1016/j.geomorph.2017.09.001>
- Sagastizábal D, Milazzo K, Jiménez F (2006) Tumulus and biomass sedimentary. *Terraeformae*, 9–29. <https://doi.org/10.1007/s11773-006-0075-3>
- Van Veenhuyse JJ (1957) *Geopaleontische en silex leisteen (Onder Water) (Intertidal) in de Rijpweg Amstelveen I (Locus typicus)*. Meded. proef. Stichts (n.s.) 11:27–30
- Vasconcelos J, Magalhães J (1991) La piallinaire (calcareous) do Portugal: as suas adjacências: análise geomorfobiogeográfica. Serviços Geológicos, Portugal, 6, Lubeca 28:66.
- Von K, Vandenberghe N, Haes J (2014) Surface texture analysis of quartz grains by scanning electron microscopy (SEM): from sample preparation to environmental interpretation. *Earth Sci Rev* 129:93–104. <https://doi.org/10.1016/j.earscirev.2013.10.013>
- Walker LM, Harten JA (1999) Distribution of recent planktonic carbonate sedimentation per: Holoc. *Am J Sci* 299(6):601–643. <https://doi.org/10.2307/29866361>
- Zafra S, García V, Martínez L, Tomé P, Alonso MA, De Ávila G, ... Moller T (2009) The quest for the Africa–Iberia plate boundary zone at the Strait of Gibraltar. *Nature and Planetary Science Lett*, 289(1–4): 13–26. <https://doi.org/10.1016/j.npl.2009.11.005>

Publisher's note Springer Nature remains neutral with regard to jurisdictional claims in published maps and institutional affiliations.

Springer Nature or its licensee (e.g. a society or other partner) holds exclusive rights to this article under a publishing agreement with the author(s) or other rightsholder(s); author self-archiving of the accepted manuscript version of this article is only permitted by the terms of such publishing agreement and applicable law.